

WALL-LESS MICROFLUIDIC CHANNELS USING 3-DIMENSIONAL RING ARRAYS

Won Chul Lee^{1,2}, Yun Jung Heo^{1,2}, Shoji Takeuchi^{1,2}

¹Institute of Industrial Science, The University of Tokyo, Japan,

²ERATO Takeuchi Biohybrid Innovation Project, Japan Science and Technology Agency, Japan

ABSTRACT

This paper presents a method to construct microfluidic channels without physical walls – wall-less microchannels. In order to minimize liquid surface areas contacted to solid walls, this method uses three dimensional ring arrays compared to the previous wall-less microfluidics based on two dimensional patterns of hydrophilic and hydrophobic areas. Thus, we can form free-standing liquid pathways surrounded by an immiscible liquid between distant rings in the ring arrays. In the experimental study, we reduced the liquid-solid interface areas per unit volume to 17.3% of that of the conventional microchannels with square cross-sections. We expect that this aspect would be important in micro/nano-fluidics, whose surface-area-to-volume ratio is extremely large.

KEYWORDS

Wall-less microfluidics, Surface-area-to-volume ratio, Ring array.

INTRODUCTION

Current micro/nano-fluidic channels have high surface-to-volume ratio and it becomes even higher as channel dimensions become reduced. [1-3] This high surface-to-volume ratio can bring both advantages and disadvantages to microfluidics and nanofluidics. It gives us a good tool to study interfaces between solid and liquid. However, large liquid surface areas contacted to physical channel walls can easily trap and release chemicals in liquid flows, thus acting as severe contamination or noise sources. [2,3]

As one of solutions, the concept of wall-less microfluidics [4-7] – microfluidic platforms without physical walls – was previously suggested. The platform (Figure 2b) utilizes surface tension to confine liquid on 2-dimensional patterns of hydrophilic and hydrophobic areas, and removes physical side-walls and/or top-covers of microfluidic channels. Since physical (solid) surfaces of covers and walls of flow-channels are replaced to an immiscible fluid (liquid or air), this method can reduce liquid surface areas contacted to solid surfaces. However, bottom surfaces of channels still remain in this microchannel, thus we can reduce liquid-solid interface areas to only ~40% of the conventional microchannels that can carry the same liquid volumes.

The present method aims to advance the concept of previous wall-less microfluidics in order to decrease the liquid-solid interface areas of microchannels. Compared to the conventional wall-less microfluidics based on 2-dimensional patterns, this method (Figure 1) uses 3-dimensional ring arrays and two immiscible liquids. The ring arrays are attracted to the liquid 1 and the substrate is attracted to the liquid 2, which is immiscible to the liquid 1. Surface tension generates free-standing pathways of the liquid 1 surrounded by the liquid 2 between separated ring microstructures. By increasing ring-to-ring distances, the liquid-solid interface area per volume can be decreased, since these free standing liquid pathways have no contact to solids except rings.

One can imagine that continuous liquid pathways will be formed when rings are close enough while discontinuous liquid drops will be formed when rings are too far. It is essential for this study to investigate ring-to-ring distances where wall-less liquid channels are formed reliably, since the ring-to-ring distances directly decide the interface-area-to-volume ratio of the present method as shown in Figure 2c. In this work, we aim to investigate the criteria of ring geometries (ring radii and ring-to-ring distances) where the liquid pathways are reliably formed, and to compare the liquid-solid interface areas per unit volume in the present microchannels with those of the conventional square microchannels and the previous wall-less microchannels.

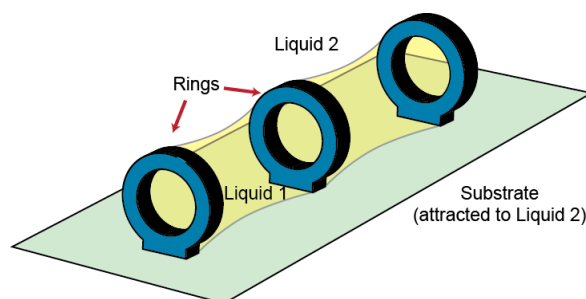
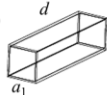
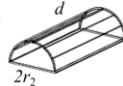


Figure 1. Conceptual illustration of the wall-less microfluidic channel with 3-dimensional ring arrays.

(a)  $a_1 = \sqrt{\frac{V}{d}} \rightarrow \frac{A_1}{V} = \frac{4a_1d}{V} = 4\sqrt{\frac{d}{V}}$

(b)  $r_2 = \sqrt{\frac{2V}{\pi d}} \rightarrow \frac{A_2}{V} = \frac{2r_2d}{V} = \sqrt{\frac{8d}{\pi V}} \cong 1.60\sqrt{\frac{d}{V}}$

(c)  $r_3 = \sqrt{\frac{V}{\pi d}} \rightarrow \frac{A_3}{V} = \frac{2\pi r_3 t}{V} = \frac{2t}{\sqrt{\pi d}} \sqrt{\frac{d}{V}} \cong \frac{3.54t}{d} \sqrt{\frac{d}{V}}$

Figure 2. Comparison of three microfluidic channels. The interface-area-to-volume ratio, A_i/V , means liquid surfaces contacted to solid walls per unit liquid volumes: (a) conventional microchannels with solid walls; (b) previous wall-less microchannels with 2-D patterns of hydrophilic / hydrophobic areas; (c) present wall-less microchannels with 3-D ring arrays.

EXPERIMENT

For a proof-of-concept, we fabricated ring arrays with various radii and ring-to-ring distances, and studied conditions where wall-less microchannels are reliably formed. We chose three kinds of ring outer radii, r_{out} (2, 4, and 8 μm), and five kinds of ring-to-ring distances (r_{out} , $1.5r_{out}$, $2r_{out}$, $2.5r_{out}$, and $3r_{out}$). We fabricated the ring arrays with a two-photon laser lithography system [8-10] (Photonic Professional, Nanoscribe GmbH). For the fabrication of 3 dimensional microstructures, this equipment uses two-photon polymerization in a negative photoresist, IP-L 780 (Photonic Professional, Nanoscribe GmbH), on a silanized glass substrate as shown in Figure 3. Figure 4 shows the scanning electron microscopy (SEM) images of the fabricated ring arrays. In order to form wall-less microchannel, we dropped the liquid 1 (hexadecane) on top of the fabricated ring array and subsequently dropped the liquid 2 (water) as shown in Figure 3.

Figure 5 shows typical results of the formation of wall-less liquid pathways in the fabricated ring arrays. Each ring appears to a microscale bar since we captured the images from the top. Successive immersion of the ring arrays with two immiscible liquids generates liquid channels and droplets. Rings close enough to each other generate continuous liquid channels while rings far from each other form discontinuous liquid drops. From the microscopic images, we could measure geometrical characteristics of liquid channels and droplets. We also verified the three dimensional shape of the liquid 1 using confocal microscopy. The cross-sectional view of the channels is circular and has no contact to substrate surfaces. Thus, we can estimate the geometrical characteristics of the liquid 1 using the microscopic images from the top.

It is important to study ring dimensions where wall-less liquid channels are reliably formed. The ring-to-ring distances which are the same as or 1.5 times of the ring radii reliably generate connected liquid channels. When the ring-to-ring distances are larger than 1.5 times of the ring radii, liquid drops are also formed. Normalized liquid volumes in Figure 6 express these results. The experimental values of liquid volumes guided by one unit ring were measured from the microscopic images, and we normalized them with the volumes of circular channels whose radii are the same as outer radii of the rings. When the distant liquid drops are formed, either the liquid volumes are small or their standard deviations are large. Thus, the maximum ring-to-ring distance which reliably generates connected liquid pathways is 1.5 times of the ring radius in our experiments.

The maximum ring-to-ring distances can be theoretically estimated by the Rayleigh instability problem [11]. The Rayleigh instability problem originally has been studied to explain why a thin cylinder of a liquid breaks into droplets. The Rayleigh instability indicates that the theoretical maximum of the ring-to-ring distances for continuous liquid pathways is 2π times of the ring radius. However, this value is much larger than the experimental value. It might be because that the Rayleigh instability problem only considers the process that a pre-formed liquid cylinder breaks into droplets while our case is the dynamic process during the liquid 2 replaces the liquid 1. Thus, the Rayleigh- instability problem is not enough to explain the formation process of the liquid channels in our case. However, the Rayleigh-Plateau instability problem can give us the upper limit of ring-to-ring distances, and it coincides well with our experiments. More detailed theoretical analysis needs to be done under the consideration of various variables, such as surface tension, solid-to-liquid interaction, liquid-to-liquid interaction, liquid viscosity, and so on.

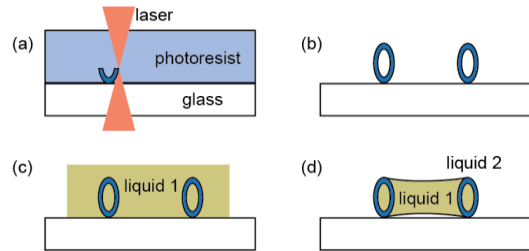


Figure 3. Ring fabrication and channel forming process: (a) direct laser writing to a negative photoresist; (b) photoresist development; (c) structure dipping in the liquid 1; (d) successive dipping in the liquid 2.

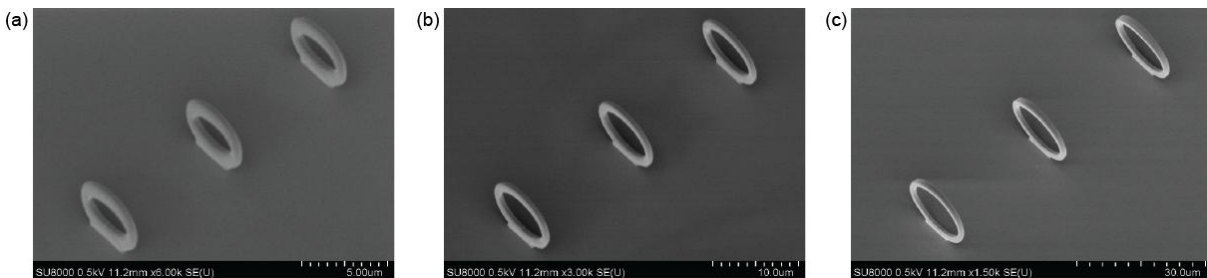


Figure 4. SEM (Scanning Electron Microscopic) images of the fabricate ring arrays with the radii of: (a) 2 μm ; (b) 4 μm ; (c) 8 μm .

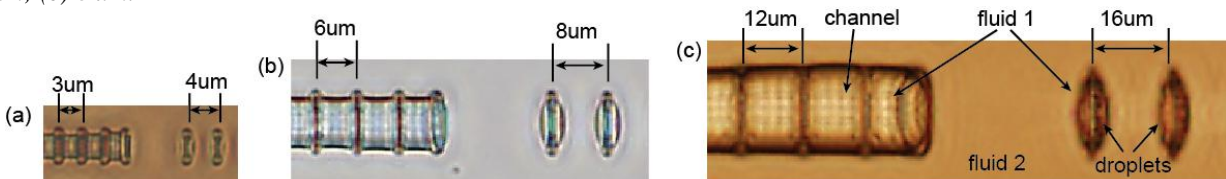


Figure 5. Microscopic images of typical wall-less microchannels with the fabricated rings whose radii are (a) 2 μm , (b) 4 μm , and (c) 8 μm .

In order to evaluate the performance of the present wall-less microchannels, we defined a variable, normalized interface-area-to-volume ratio, which is conceptually similar to the normalized surface-area-to-volume ratio. We can obtain the interface-area-to-volume ratio of any given channel from the area of liquid-solid interfaces and liquid volumes. Then, we normalized the interface-area-to-volume ratio with that of the conventional square channel which can carry the same liquid volume as that of the circular channel. Thus, the defined value of the conventional square channel is 1, and the defined value is less than 1 when the liquid area contacted to solid surfaces is reduced. For example, the value is 0.4 in the previous wall-less microchannels using 2-dimensional patterns of hydrophilic / hydrophobic areas. We calculated the normalized interface-area-to-volume ratios of the present wall-less microchannel, and the present method ($r_{out} = 2\mu\text{m}$ and $d_r = 3\mu\text{m}$) reduced the liquid-solid contact area to 17.3% of that of the conventional microchannels with square cross-sections. This value is smaller than that of the previous wall-less microchannels (40%), and can be further reduced by changing ring dimensions, surface treatments, and/or liquid compositions. Thus, this work verifies the feasibility that the present method can reduce the liquid areas contacted to solid surfaces in microchannels.

In conclusion, this paper describes wall-less microfluidics using 3-dimensional ring arrays and two immiscible fluids, and experimentally shows that the present device can reduce the liquid-solid interface areas compared to the previous wall-less microfluidics. We envision that this point would be important in the field of nanofluidics, whose surface-area-to-volume ratio is extremely high. Additionally, we expect that this method can be applied for sacrificial molds of the polymeric channel fabrication and/or critical components of switchable microfluidics.

REFERENCES

- [1] G.M. Whitesides, *The origins and the future of microfluidics*, Nature, 442, pp.369, (2006).
- [2] G.M. Whitesides, *What comes next?*, Lab on a Chip, 11, pp.191, (2011).
- [3] J. Eijkel and A. van de Berg, *Nanofluidics: what is it and what can we expect from it?*, Microfluidics and Nanofluidics, 1, pp.249, (2005).
- [4] L. Wang and A. Lee, *Wall-less microfluidics with on-site MHD pumps for continuous flow control*, Proc. Bio Micro and Nanosystems Conference 2006, IEEE, San Francisco, California, USA, pp.95, (2006).
- [5] B. Zhao, J.S. Moore, and D.J. Beebe, *Surface-directed liquid flow inside microchannels*, Science, 291, pp.1023, (2001).
- [6] A. Nag, B.R. Panda, and A. Chattopadhyay, *Performing chemical reactions in virtual capillary of surface tension-confined microfluidic devices*, Pramana-Journal of Physics, 65, pp.621, (2005).
- [7] A. Banerjee, E. Kreit, Y. Liu, J. Heikenfeld, and I. Papautsky, *Reconfigurable virtual electrowetting channels*, Lab on a Chip 12, pp.758, (2012).
- [8] J.H. Atwater, P. Spinelli, E. Kosten, J. Parsons, C. Van Lare, J. Van de Groep, J. Garcia de Abajo, A. Polman, and H.A. Atwater, *Microphotonic parabolic light directors fabricated by two-photon lithography*, Applied Physics Letters, 99, pp.151113, (2011).
- [9] M. Thiel, J. Fischer, G. von Freymann, and M. Wegener, *Direct laser writing of three-dimensional nanostructures using a continuous-wave laser at 532nm*, Applied Physics Letters, 97, pp.221102, (2010).
- [10] I. Staude, M. Thiel, S. Essig, C. Wolff, K. Busch, G. von Freymann, and M. Wegener, *Fabrication and characterization of silicon woodpile photonic crystals with a complete bandgap at telecom wavelengths*, Optics Letters, 35, pp.1094, (2010).
- [11] F. Charru and P. de Forcrand-millard, *Hydrodynamic Instabilities*, Cambridge University Press, pp.64, (2011).

CONTACT

Prof. Shoji Takeuchi 81-3-5452-6650 or takeuchi@iis.u-tokyo.ac.jp

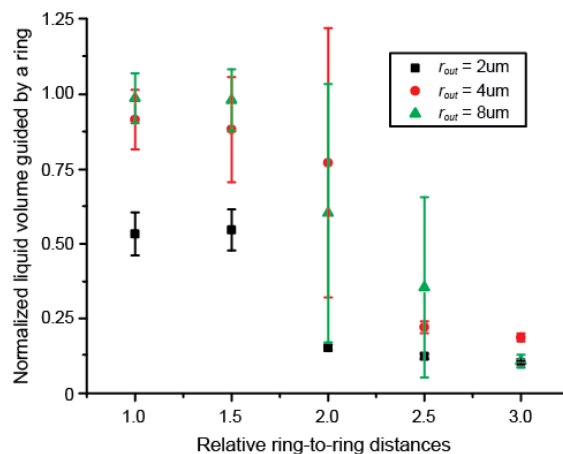


Figure 6. Normalized liquid volume guided by each ring for varying ring radii and ring-to-ring distances.